



# Mapping grape production parameters with low-cost vehicle tracking devices

J.-P. Gras<sup>1</sup> · S. Moinard<sup>1</sup> · Y. Valloo<sup>1</sup> · R. Girardot<sup>1</sup> · B. Tisseyre<sup>1</sup>

Accepted: 31 January 2024

© The Author(s), under exclusive licence to Springer Science+Business Media, LLC, part of Springer Nature 2024

## Abstract

This study presents a method based on retrofitted low-cost and easy to implement tracking devices, used to monitor the whole harvesting process in viticulture, to map yield and harvest quality parameters in viticulture. The method consists of recording the geolocation of all the machines (harvest trailers and grape harvester) during the harvest to spatially re-allocate production parameters measured at the winery. The method was tested on a vineyard of 30 ha during the whole 2022 harvest season. It has identified harvest sectors (HS) associated with measured production parameters (grape mass and harvest quality parameters: sugar content, total acidity, pH, yeast assimilable nitrogen, organic nitrogen) and calculated production parameters (potential alcohol of grapes, yield, yield per plant) over the entire vineyard. The grape mass was measured at the vineyard cellar or at the wine-growing cooperative by calibrated scales. The harvest quality parameters were measured on grape must samples in a commercial laboratory specialized in oenological analysis and using standardized protocols. Results validate the possibility of making production parameters maps automatically solely from the time and location records of the vehicles. They also highlight the limitations in terms of spatial resolution (the mean area of the HS is 0.3 ha) of the resulting maps which depends on the actual yield and size of harvest trailers. Yield per plant and yeast assimilable nitrogen maps have been used, in collaboration with the vineyard manager, to analyze and reconsider the fertilization process at the vineyard scale, showing the relevance of the information.

**Keywords** Precision viticulture · GNSS · Geospatial data processing · Nitrogen fertilization

## Introduction

Detailed and precise knowledge of production parameters (yield, quality, health status, etc.) is the basis for analyzing the effect of any agricultural practice. Fine mapping of production parameters, either yield or quality parameters, makes it possible to identify the origin of observed variability, whether associated with environmental factors or with agricultural

---

✉ J.-P. Gras  
jean-philippe.gras@supagro.fr

<sup>1</sup> ITAP, Univ Montpellier, Institut Agro, INRAE, 2 Place P. Viala, 34060 Montpellier, France

practices, such as seeding, fertilization and irrigation among others (Simmonds et al., 2013). Yield and harvest quality parameters mapping requires specific sensors (when they exist), mounted on harvesting machines (Birrell et al., 1996; Momin et al., 2019). These sensors are sometimes costly and/or cumbersome to calibrate. Yield sensors are particularly common in arable crops, but they are not widely used, at least in France, for yield mapping. This is mainly due to calibration constraints required to obtain precise yield data (Lachia et al., 2021) and also for cost reasons (Longchamps et al., 2022). Remote sensing has been proposed to indirectly estimate field yield and its variability in viticulture. Most common approaches hypothesize that plant yield is correlated with photosynthetically active biomass at a key phenological stage of the crop (Longchamps et al., 2022). These approaches still need an important calibration step, which is almost block specific to relate vegetative index derived from remote sensing images with actual yield. Therefore, they are quite difficult to implement, and to our knowledge, there is still no commercial services available based on such an approach. As a result, spatial knowledge of yield and its variability is still a difficult variable for growers and advisors to obtain. Regarding harvest grape quality parameters, despite a few attempts (Baguena et al., 2009, Bramley et al., 2011), the situation is even worse. Indeed, these are parameters for which on-line measurements on a grape harvesting machine remain very difficult, and to our knowledge, there is still no grape harvesting machine able to measure grape quality parameters on the go. This is particularly problematic since many studies have shown that knowledge of harvest quality parameters is very important in terms of decision-making, since it contributes to the added value of the product and defines the entire wine-making process (McClymont et al., 2012). This difficulty to get yield and harvest quality parameters mapping is an important limitation for precision viticulture to be adopted.

As an alternative, low-cost methods using Global Navigation Satellite System (GNSS) tracking devices (TDs) have been developed for yield mapping in agriculture. Schueller et al. (1999) and Momin et al. (2019) have developed reliable methods, based on commercial TDs, to respectively generate yield maps of hand-harvested citrus and sugar cane. More recently, Bayano-Tejero et al. (2024) proposed their own TDs with an on-board weighing system to map olive production.

Momin et al. (2019) showed that it was possible to allocate sugar cane yield data measured at the receiving platform to a within block level from the geolocation of two machines: the harvester and the harvest trailer. Although it contained some inaccuracies, this approach was proven to be relevant. Moreover, it has the advantage of (i) being integrated into the organization and equipment of current harvesting methods, which allows for easy and rapid deployment as a retrofit, (ii) limiting operations regarded as tedious, such as the maintenance and calibration of on-board sensors and (iii) mapping all information collected at the reception dock without having to add additional specific sensors.

The approach proposed by Momin et al. (2019) is of great interest in viticulture. Indeed, many parameters (grape mass, sugar content, pH, total titratable acidity, yeast assimilable nitrogen content, etc.) are routinely carried out at the winery when the harvest is delivered. A total traceability of the harvesting process would therefore make it possible to reallocate this information to a within field level. To our knowledge, the use of TDs to map all harvest parameters commonly measured at the winery has never been tested in viticulture.

The objectives of this work are therefore (i) to implement and study the use of low-cost commercial TDs to generate production parameters mapping for viticulture. It proposes to investigate the applicability of the approach developed by Momin et al. (2019) to vineyard mapping. Compared to the work of Momin et al. (2019), the viticultural case is more complex since several harvesting trailers can operate simultaneously on the same harvesting

site. The question that this study seeks to address is then to propose, design and validate a specific algorithm accounting for this specificity and to verify whether its application allows a total traceability of the harvest operations, (ii) to verify that only the time and geolocation information of vehicles equipped with low-cost tracking TDs, is sufficient to reconstruct agronomical relevant within-block maps of harvest parameters in viticulture, (iii) to identify the limit of the approach in terms of maintenance but also in terms of spatial footprint (resolution) of the maps, (iv) to verify whether the provided maps are relevant enough for the growers or the advisers to support decision and new management practices. To this end, a specific experiment was adopted with the vineyard manager based on the obtained maps.

## Materials and methods

### Study sites

The study took place in a vineyard estate located in the south of France, near Montpellier (Villeneuve-lès-Maguelone, WGS84—43.532300° N, 3.864230° E) during the 2022 harvest season (August–September). The area of the vineyard estate is 30 ha organized into 51 different blocks. A block refers to a section of the vineyard with uniform grape variety, rootstock, training system, same date of plantation, etc. A block commonly corresponds to a management unit. Harvesting was performed mechanically with a grape harvesting machine (Pellenc, Pertuis, France) mounted with two hoppers of 600 kg grape capacity each. During the harvest, once the harvesting machine was full, the hoppers were emptied into trailers towed to tractors that transferred the grapes to the vineyard cellar or to a wine-growing cooperative depending on the variety. Depending on the distance of the blocks from the winery, 2 to 3 trailers (with a maximum capacity of 3500 kg of grapes each) were used to ensure the continuity of the harvest operation.

### Measurement of production parameters

Two measurement protocols were used depending on where the grapes were brought in: the vineyard cellar or the cooperative.

At the vineyard cellar, the trailers were systematically weighed. Harvest trailers are weighed in one single scale to get the mass of grapes. The mass of grapes is equal to the mass of the full harvest trailer minus the mass of the empty harvest trailer (this mass is measured at the beginning of the harvest season). The scale also registers the weighing time. In addition, a sample of grape must (30 centiliters) was collected inside the trailer and sent to a commercial laboratory specialized in oenological analysis (Institut Coopératif du Vin, Montpellier, France) to measure harvest quality parameters: sugar content (SC), total acidity (TA), pH, yeast assimilable nitrogen (YAN), organic nitrogen (ON). Given the filling of the trailer by the harvesting machine, the shakings during transport, and the precautions taken during sampling, this must sample is considered to be representative of the must contained in the whole trailer. After weighing and sampling, the harvest trailer may return to the field to get new grapes from the grape harvester or come back to the vineyard hangar.

At the wine growing cooperative, the harvest trailers are weighed at their arrival, when they are full of grapes, and at their departures when they are empty. After departure, the

harvest trailers return to the field to get new grapes or return to the vineyard hangar. The potential alcohol percentage was calculated from sugar content but no additional must analysis was performed.

For both, vineyard cellar and wine growing cooperative, the accuracy of the calibrated scales mass measurement is  $\pm 50$  kg. The accuracy of the weighing scales time measurements is  $\pm 1$  s.

## Geolocation of the vehicles

Each vineyard vehicle was equipped with a real-time kinematic (RTK) GNSS receiver embedded in a commercial tracking device (TD) manufactured by Samsys (Lille, France). A static RTK base, part of the Centipède RTK Network (Ancelin et al., 2022; INRAE, 2019) was installed near the winery, at a maximum distance of 5 km from any of the study blocks.

This type of TD was chosen because of (i) its low price (around 400 €/device), (ii) its accuracy ( $\pm 50$  mm with RTK GNSS), (iii) its acquisition frequency (data recorded at 1 Hz), (iv) its ease of implementation (it is attached to the machine by a strong magnet system), (v) the accessibility of the data which are sent back by general packet radio service (GPRS) protocol to a server accessible via an application programming interface (API), and (vi) its battery autonomy, given to be around 2 weeks by the manufacturer for an intensive use. Four TDs were used during the whole season; with one positioned on the grape harvester and three TDs positioned on each of the three harvest trailers.

The receivers used can either run on batteries or on the tractor power supply. However, in the case of TDs positioned on the harvest trailers, their goal was to track and record the location of the grapes crop during harvest. Considering that tractor/trailer pairing could change during a harvest day, TDs must be positioned on the trailer and not on the tractor to avoid any uncertainty. Therefore, for TDs on trailer, plugging the device into the tractor power supply was not easy and complicated to set up and manage. As a result, these TDs were running exclusively on batteries. For TD on harvester, it was plugged into the harvester power supply.

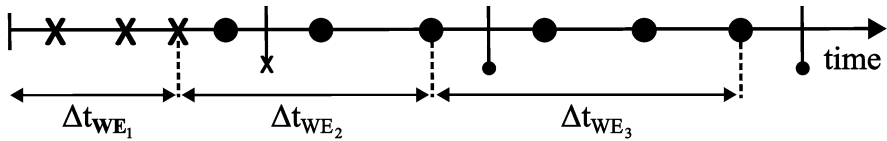
## Spatial reallocation of data measured at the reception dock

The method relies only on time and geolocation measurements of the vehicles involved in the harvesting. The methodology, summarized in Fig. 1, is based on two types of events over the time:

A weighing event (WE); when a harvest trailer is weighed at the winery or at the cooperative,

A filling event (FE); when the grape harvester fills a harvest trailer.

Regarding WE, each weighing event  $WE_i$  ( $i = 1 \dots N_{WE}$ , with  $N_{WE}$  the number of WE) is defined as a vector.  $WE_i = \{t_i, id_i, m_i, qp_i\}$  where  $t_i$  is the weighing time given by the scale clock,  $id_i$  is the identity of the harvest trailer ( $id_i = 1, 2, 3$ ) weighed,  $m_i$  is the grape mass and  $qp_i$  is a vector which characterizes harvest quality parameters measured on a must sample from the harvest trailer.  $qp_i = \{SC_i\}$  if the trailer is unloaded at the wine-growing cooperative and  $qp_i = \{SC_i, TA_i, pH_i, YAN_i, ON_i\}$ ; if the trailer is unloaded at



**Legend :**

- FE of harvest trailer 1      | WE of harvest trailer 1
- X FE of harvest trailer 2      X WE of harvest trailer 2

**Fig. 1** Chronology of events during a harvest day with three WEs and 2 harvest trailers. Step 1: Association of harvest trailers to WEs and detection of FEs. Step 2: estimation of the harvesting time intervals ( $\Delta t_{WE_1}$ ,  $\Delta t_{WE_2}$ ,  $\Delta t_{WE_3}$ ) associated with the different WEs from WEs and FEs chronology

the vineyard cellar. The identity of the harvest trailer  $id_i$  associated to the weighing event  $WE_i$  is determined as follows. First, the minimum Euclidean distance  $d_j$  between the locations  $S_j$  of each harvest trailer  $j$  (with  $j = 1, 2, 3$ , because there are three harvest trailers) during an interval of  $[t_i - \Delta t_s, t_i + \Delta t_s]$ , and the scale location  $S_C$  is calculated for each harvest trailer:

$$d_j = \text{minimum}(d(S_j([t_i - \Delta t_s, t_i + \Delta t_s]), S_C)) \tag{1}$$

Then, the harvest trailer identity  $id_i$  associated with the  $WE_i$  corresponds to the harvest trailer  $j$  with the smallest minimum distance  $d_j$  to the scale during the interval  $[t_i - \Delta t_s, t_i + \Delta t_s]$  at the condition that this distance is inferior to a threshold distance  $s_{WE}$  (maximum distance between harvest trailers and the scale during a WE). These conditions are sufficient to associate the right harvest trailers with measurements because harvest trailers came directly from the field and don't stay near the scale while another trailer is weighed. Indeed, the value of  $\Delta t_s$  is chosen in order that during the interval  $[t_i - \Delta t_s, t_i + \Delta t_s]$  of the measurement, only one harvest trailer mass is measured. For this purpose,  $\Delta t_s$  need to be inferior to the minimum duration between 2 mass measurements over the entire harvest season.

Regarding FE, each filling event  $FE_i$  ( $i = 1 \dots N_{FE}$ , with  $N_{FE}$  being the number of FE) is defined as a vector;  $FE_i = \{t_i, id_i\}$  where  $t_i$  is the filling time from harvester into the trailer and  $id_i$  is the identity of the harvest trailer filled ( $id_i = 1, 2, 3$ ).  $FE_i$  are detected when two conditions are satisfied. The first condition uses the spatial proximity between the grape harvester and the harvest trailers during filling. The second condition accounts for the minimum duration required to empty the grape harvester into a harvest trailer. This second condition was added in order to differentiate FE from simple machine crossings (e.g. when the grape harvester ends a vine row and passes close to a harvest trailer waiting on the border of the vine block).

$$d(S_j(t), S_H(t)) \leq s_{FE} \forall t \in [t_i, t_i + \Delta t_i] \text{ and } \Delta t_i \geq \Delta t_{FE} \tag{2}$$

where,  $S_j(t)$  and  $S_H(t)$  are respectively the location of the harvest trailer  $j$  and of the grape harvester at time  $t$ ,  $t_i$  is the filling time of the  $FE_i$  when both conditions are satisfied.  $s_{FE}$  is a threshold distance (the maximum Euclidean distance between grape harvester and

harvest trailer during a FE).  $\Delta t_{FE}$  is a threshold duration corresponding to the minimum time duration required by the grape harvester to fill an harvest trailer.

As the capacity of a harvest trailer is larger than the storage capacity of the grape harvester, several FEs can be carried out with the same trailer before a WE is observed. Therefore, the algorithm uses the whole chronology of FEs and WEs to estimate harvesting time intervals  $\Delta t_{WE_i}$  associated to  $WE_i$  (Fig. 1). For example, in Fig. 1,  $\Delta t_{WE_1}$  is associated with the first WE. For each  $\Delta t_{WE_i}$ , harvester locations (points) are known. Then, at the end of the reallocation, each harvester location (point) is associated with a  $WE_i$ . The sector covered by the harvester locations inside a block, associated with a  $WE_i$ , will be called a harvest sector and noted  $HS_i$ .

The delimitation of each harvest sector  $HS_i$  and the calculation of its corresponding area  $A_i$  are performed in four steps:

1. First, harvester locations were filtered using the blocks data boundaries in order to keep only the intra-block harvester locations.
2. Second, a density-based spatial clustering of applications with noise (DBSCAN) algorithm (Ester et al., 1996) was used to identify geographical clusters of harvest machine locations within blocks. By using the convex hulls of these clusters, intra-blocks harvest zones are defined. This step is necessary in the case that the blocks are partially harvested by the harvest machine (for example, if some rows are harvested by hand, or if the decision of not harvesting a specific zone inside a block has been made). In the case that a block is totally harvested, the resulting intra-block harvest zone is equal to the block.
3. Third, a Voronoï tessellation (Arnaud & Emery, 2000) was used to define the spatial footprint (Voronoi polygon) of each grape harvester location (point) within the intra-block harvest zones. At this stage, each Voronoï polygon is associated with an intra-block harvester location (point) and its associated WE.
4. Finally, the Voronoï polygons corresponding to the same  $WE_i$  are merged to form a unique entity, delimiting the harvest sector  $HS_i$ . The area  $A_i$  (in ha) of the harvest sector  $HS_i$  is defined by  $A_i = \sum_{k=1}^{K_i} A_k$ .  $A_k$  (in ha) is the area of the Voronoï polygons associated to the point of index  $k$  and  $K_i$  is the number of points of the grape harvester path associated with a  $WE_i$ .

## Production parameters mapping

Yield  $Y_i$  in  $t\ ha^{-1}$ , associated with a harvest sector  $HS_i$ , was then calculated as indicated by the following equation:

$$Y_i = \frac{m_i}{A_i} \quad (3)$$

where,  $m_i$  and  $A_i$  are respectively the mass of grape (in t) and the area (in ha) associated with the harvest sector  $HS_i$ . Yield per plant ( $YieldPP_i$  in  $kg\ plant^{-1}$ ) of each specific harvest sector  $HS_i$  is also calculated. This variable has an interesting agronomic value, it corresponds to the mass of grapes ( $m_i$ ) divided by the number of productive plants ( $NP_i$ ) of the considered  $HS_i$ :

$$YieldPP_i = \frac{m_i}{NP_i} \quad (4)$$

In a harvest sector, the number of productive plants is equal to the original number of plants ( $NO_i$ ), at the time of the plantation, minus the number of unproductive plants ( $NU_i$ ):

$$NP_i = NO_i - NU_i \quad (5)$$

The original plants number  $NO_i$  is equal to:

$$NO_i = \sum_{k=1}^{k=K_i} (d_k \times A_k) \quad (6)$$

With  $A_k$  (in ha), the area of the Voronoï polygon associated to the harvester location point of index  $k$  and  $K_i$  the number of points of the grape harvester path associated with a  $WE_i$ .  $d_k$  is equal to the original planting density (number of plants by hectare) of the block in which the point of index  $k$  is located. In the study, for most of the cases, harvest sectors are within a unique block ( $d_k$  is then the same for all points), but in some cases a harvest sector may cover more than one block ( $d_k$  may differ if the blocks planting densities are different). In the vineyard studied, unproductive vines were geolocalized manually over the whole vineyard using a RTK GNSS receiver, of accuracy 1–5 cm. The number of unproductive vines ( $NU_i$ ) inside a specific harvest sector is estimated from the localization of unproductive vines and the localization of the harvest sector.

Concerning harvest quality mapping, each harvest sector  $HS_i$  is associated with a  $WE_i$  and its  $qp_i$  vector. For some harvest sectors  $HS_i$ , the quality parameters available will be  $qp_i = \{SC_i\}$ ; if the grapes harvested inside this  $HS_i$  were unloaded at the wine-growing cooperative; or  $qp_i = \{SC_i, TA_i, pH_i, YAN_i, ON_i\}$ ; if the grapes harvested inside this  $HS_i$  were unloaded at the vineyard cellar. The potential alcohol  $PA_i$  (in % v v<sup>-1</sup>) associated with a harvest sector  $HS_i$  is calculated by the following equation:

$$PA_i = \frac{SC_i}{16.83} \quad (7)$$

where  $SC_i$  is the sugar content (in g l<sup>-1</sup>) associated with the harvest sector  $HS_i$ .

## Implementation of the methods

The algorithm was implemented using the Python language (Van Rossum & Drake, 2009). The access to geospatial data from the Samsys API was done with the request library (Chandra & Varanasi, 2015). The geospatial data processing was made with the Geopandas library (Jordahl, 2014). Geometric operations (intersection, Voronoï tessellation) were performed with the shapely library (Gillies et al., 2007). The DBSCAN algorithm was implemented via scikit-learn machine learning library (Pedregosa et al., 2011). Dynamic html maps were made using the folium library (python-visualization, 2020) while static maps were made with QGIS software (QGIS Development Team, 2009).

## Real use case definition

The spatialisation of the viticultural variables measured in this work is original. Our working hypothesis was that these new sources of information would necessarily lead to a desire from the vineyard manager to improve certain agricultural practices.

In order to validate this hypothesis, the different maps obtained were printed and presented to the vineyard manager. No specific method was used for this step; the aim was

simply to observe the vineyard manager and identify any surprises or concerns such as unusually low or high sector values. The meeting also involved noting the hypotheses that were formulated by the vineyard manager to explain sectors with surprising values and identifying whether agronomic reasoning could be considered to change some agricultural practices in order to address any observed potential issues.

Once identified and analyzed, potential site-specific management practices were formalized with simple rules or classes value like: if X variable is Low and Y variable is High then a specific management ( $M_i$ ) should be performed on the considered sector. A second step was considered to validate the application, the rules but also the thresholds (class) used to define the different levels (High, Low, etc.). This validation was performed in four steps: (i) compare the overall reasoning and rules to the literature knowledge, (ii) validate the classes and rule conclusions with an agricultural advisor, (iii) perform a final validation by the vineyard manager, (iv) validation by the latter of the conclusions in the form of a map and the resulting management units.

## Results

The geolocation data of all the vehicles (1 grape harvester and 3 harvest trailers) were successfully recorded for the entire 2022 harvesting season and for the whole vineyard estate. As it is difficult to visualize this information over the whole vineyard, an example of the path of the grape harvester within a few blocks is shown Fig. 2. In total, there have been 87 WEs during the harvest season. The average mass of grapes per trailer was 2420 kg and a total of 208 t of grapes were harvested in the vineyard over a period of 5 weeks (17 days of harvesting). Table 1 summarizes main statistics on the duration between harvest trailer weighings at the vineyard cellar and at the wine growing cooperative. The mean time between two weighings is 38 min. This duration is approximately the duration necessary to fill a trailer. In a few cases, the duration between two harvest trailer weighings is short; the minimum duration is 3 min. Based on these statistics,  $\Delta t_s$  was chosen equal to 1 min in order to properly associate the harvest trailer to a weighing event at the vineyard cellar ( $\Delta t_s$  need to be inferior to the minimum duration between two weighing events: 3 min). Based on observed results, the maximum distance between tractor trailers and the scale during a WE was about 10 m. Indeed, even if RTK GNSS sensors are used with a centimetric accuracy, in presence of buildings (which are present at the scale location), the accuracy of the sensors is sometimes altered (because of multipath errors). The  $s_{WE}$  parameter was then chosen equal to 10 m. Using these parameters, each WE was successfully associated with the right harvest trailer during the entire harvest season.

During FE, the maximum observed distance between the TD mounted on the harvester and the TD mounted on the harvest trailer was equal to 15 m;  $s_{FE}$  was then chosen equal to 15 m to be sure to not miss filling events. The minimum duration required by the harvester to fill a harvest trailer during the entire harvest season was equal to 1 min;  $\Delta t_{FE}$  was then chosen equal to 1 min. Using these parameters, the FEs were correctly detected based on harvest machines geolocation and time information alone. Up to 4 FEs were recorded to fill a trailer before its departure from the block to the winery. No errors or uncertainties were detected, which allowed the allocation of each WE to harvest sectors based on WEs and FEs chronology.





**Fig. 2** Example of intra-blocks grape harvester path recorded within some vineyard blocks over the harvesting season. The black lines correspond to block boundaries. Each color corresponds to a harvest sector associated with a WE. Mass of grapes and harvest time duration associated with WE<sub>s</sub> are displayed on the map

**Table 1** Statistics of the duration in minutes between two harvest trailers weighings during the entire 2022 harvest season

Mean (min)	Median (min)	Minimum (min)	Maximum (min)	Standard deviation (min)
38	31	3	137	30

Figure 2 shows an example of the grape harvester path during harvesting; each color corresponds to a specific harvest sector (HS) associated to a WE. Figure 2 highlights how measurements performed on the grape must at the winery can be traced back to within block locations. It also highlights the relevance of the geolocation of the grape harvester obtained with the RTK-TD, where each harvesting row could be properly identified. Moreover, very few outlier positioning data were detected over the season.

Figure 3a shows an example of the result of the Voronoï tessellation on the recorded data. The quality of the geolocation data makes it possible to estimate with accuracy the harvest sector areas. The total harvested area was found to be 26.2 ha which corresponded very well with the real area harvested mechanically. The mean yield of the whole vineyard estate was estimated to be 7.9 t ha<sup>-1</sup>. Figure 3b shows the histogram of the area of harvest sectors (i.e. area corresponding to a WE). The average harvest sector was 0.3 ha. The harvest sector areas were highly variable, ranging from 0.05 to 1.3 ha.

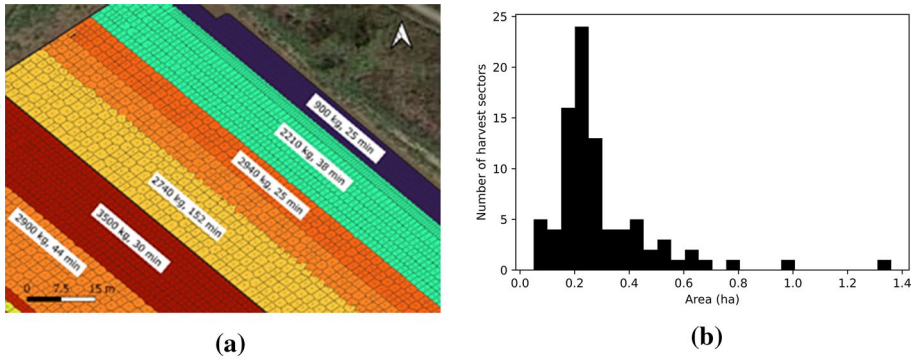


**Fig. 3** **a** Voronoi tessellation derived from the geolocation of the grape harvester. Each polygon color corresponds to a weighing event (WE). Boundaries of blocks are in black. Mass of grapes and harvest time duration associated with WE<sub>s</sub> are displayed on the map. **b** Histogram of the area of harvest sectors as identified by the methodology over the whole vineyard. The bars widths are equal to 0.05 ha



**Fig. 4** Yield per plant (YieldPP) map of harvest sectors observed for the whole vineyard estate. Each color corresponds to a yield quartile computed at the vineyard estate scale

The proposed methodology allows the generation of maps for each measured production parameter. Yield, yield per plant (YieldPP), sugar content (SC) and potential alcohol (PA) maps cover the whole vineyard estate as trailer mass and sugar content were measured at the vineyard cellar and at the wine-growing cooperative. Maps relative to quality parameters such as total acidity, pH, yeast assimilable nitrogen and organic nitrogen don't cover the whole estate because these quality parameters were measured only for the trailers





**Fig. 5** Yeast assimilable nitrogen (YAN) map of harvest sectors. Each color corresponds to a yield quartile calculated at the vineyard estate scale



**Fig. 6** Potential alcohol map of harvest sectors. Each color corresponds to a yield quartile calculated at the vineyard estate scale

which delivered the grapes at the vineyard estate (and not at the cooperative). Figures 4, 5 and 6 show respectively the yield per plant (YieldPP), the yeast assimilable nitrogen (YAN) and the potential alcohol (PA) maps derived from the proposed methodology for the whole vineyard estate.

To simplify the representation, the different harvest sectors were classified in 4 quartile classes. Each map highlights the variability that was observed both at the intra-block level and at the inter-block level. For example, the yield per plant of the harvest sectors ranged from 0.5 to 5.5 kg plant<sup>-1</sup>, the YAN from 59 to 281 mg l<sup>-1</sup> and PA from 7.5 to 16.9% v v<sup>-1</sup>. An accurate description of the data and an access to these data is available in Gras et al. (2023).

## Results on the use case

The presentation of the maps to the vineyard manager (VM) led him to question the relevance of the nitrogen fertilization as it has been performed over all the fields for several years. Indeed, until now, the VM applied a uniform 50 kg of nitrogen per hectare (kgN ha<sup>-1</sup>) in spring. Two sources of information provided by the project have led him to question this uniform management: the yield variability and the yeast assimilable nitrogen (YAN) variability. It should be noted that the significant increase in the nitrogen fertilizer price over the last 2 years and the objective to substitute the classical solid chemical fertilizers with more targeted application practices like foliar liquid nitrogen application (Gutiérrez-Gamboa et al., 2022) have also contributed to consider changes in nitrogen management practices.

Figure 7 summarizes the decision rules formulated by the VM on the basis of observed yield and YAN values for each harvest sector. It shows that YAN is an important input variable for nitrogen modulation. Indeed, the literature considers that below 160 mg l<sup>-1</sup>, the YAN in the grape must is not high enough for wine fermentation to work properly. The literature also shows that it is difficult to directly relate nitrogen fertilization applied during the season

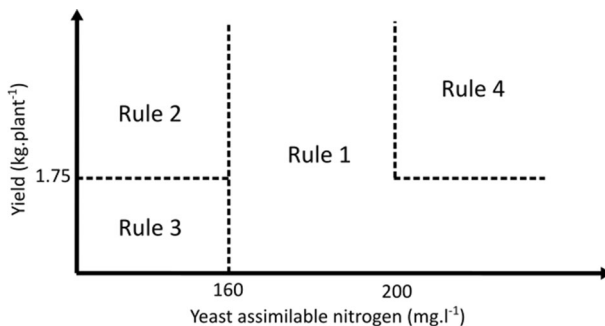


**Fig. 7** Decision rules defined by the vineyard manager on the basis of yield and Yeast Assimilable Nitrogen (YAN), the different rules aim at managing the nitrogen fertilization of the different sectors. Rule 1: nitrogen fertilization practice should be kept as it was before, Rule 2: reduction of nitrogen spring fertilization to 30 kgN ha<sup>-1</sup> and addition of a foliar liquid fertilization with 20 kgN ha<sup>-1</sup> at veraison stage, Rule 3: review fertilization and management practices (addition of organic matter, legumes, irrigation, etc.) and possibly supplement with foliar liquid fertilization with 20 kgN ha<sup>-1</sup> at veraison stage, Rule 4: spring fertilization can be reduced to 30 kgN ha<sup>-1</sup>

(in spring) with YAN of the must (Verdenal et al., 2015). However, some studies have highlighted a direct linear relationship between an increase in YAN and the amount of nitrogen applied on the leaves a few weeks before harvest, at veraison (Verdenal et al., 2015). On the basis of this knowledge, the rules formulated by the VM clearly aim to increase nitrogen efficiency by considering a reduction in the doses applied in spring when the yield is high enough and by proposing a targeted foliar application to guarantee a YAN value higher than  $160 \text{ mg l}^{-1}$ . In the peculiar conditions of the vineyard a yield of  $1.75 \text{ kg vine}^{-1}$  was considered by the VM as a limit under which the vines could experience vigor issues either due to nitrogen or water availability. The different rules account for these considerations:

✓Rule 1: highlights sector where the situation is as expected in terms of YAN. Yield can be too low but not because of nitrogen availability. Without any other information, it was decided to keep the fertilization as it was ( $50 \text{ kgN ha}^{-1}$  applied over the soil in spring). Note also that for some sectors, YAN was not available; in this case, and in the absence of any other information, the rule 1 applies, maintaining the fertilization that has been applied on the farm over the last years,

✓Rule 2: highlights sector with a correct yield but a too low YAN. In this case, the vineyard manager decided to decrease spring fertilization to  $30 \text{ kgN ha}^{-1}$  while adding a target foliar application ( $20 \text{ kgN ha}^{-1}$ ) a few weeks before harvest to increase YAN in grape must,

✓Rule 3: highlights sectors with the worst situations; low yield and low YAN. They require more in-depth agronomical analysis (sanitary issues, soil, organic matter, water capacity, etc.) before a decision can be taken. This will undoubtedly lead to a rethinking of vine management (cover crop, irrigations, etc.). However, in the short term, the vineyard manager would implement a target foliar application ( $20 \text{ kgN ha}^{-1}$ ) a few weeks before harvest to make sure to increase YAN in must.

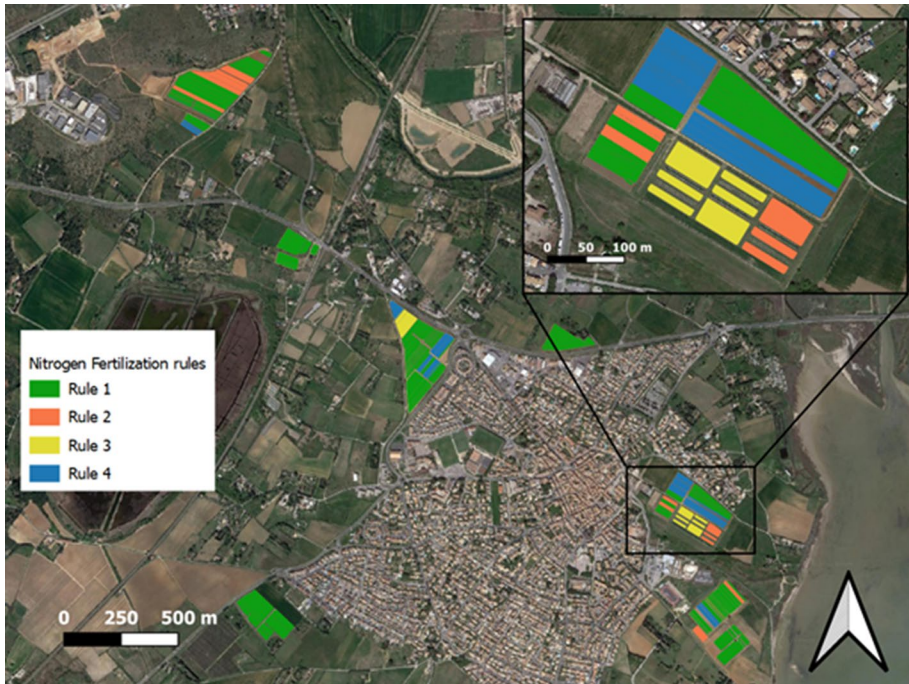
✓Rule 4: highlights sectors with high vigor and may be a high nitrogen availability. The vineyard manager considers to decrease significantly nitrogen fertilization in this case (only  $30 \text{ kgN ha}^{-1}$  in spring).

Figure 8 shows the sectors concerned by a change in fertilization practices. Note that for the majority of sectors (70% of the vineyard area), Rule 1 applies which means that the fertilization remains unchanged or that YAN information was not available. Approximately 12%, 5%, 13% of the area is affected by rules 2, 3 and 4 respectively, which corresponds to a significant change for the vineyard manager. The amount of nitrogen applied goes from 1300 to 1267  $\text{kgN}$  over the whole vineyard with the application of the rules. This new management strategy of the fertilization applied in 2023 does not really result in a reduction in the amount of nitrogen but more in improving the efficiency of the nitrogen applied.

## Discussion

During the whole harvest season, the method was able to map the origin of all yield and grape quality data recorded at the winery. This demonstrated: (i) the interest of low-cost commercial Tracking Devices (TDs) for mapping as no producer intervention was necessary during the harvest, apart from reloading the batteries every fortnight, (ii) the relevance of the proposed algorithm which, even with the presence of 3 trailers, could be automated and avoided ambiguities in the allocation of harvest data and, (iii) the retrofitting possibility





**Fig. 8** Site specific nitrogen application map derived from information obtained over each sector and the rules combining YAN and yield

of the approach on existing equipment without any additional workload for the machine operators, either for calibration or for maintenance issues (except for battery reloading).

The approach naturally has limitations since the spatial resolution of the measured data ranged from 0.05 to 1.3 ha. This variability could be explained by: (i) organizational constraints when, for example, at the end of the day, a harvest trailer returned to the winery while not completely full. In this case, the sector area assigned to the measurements will be small since it corresponds to a small harvested sector, (ii) the actual yield of the block, i.e. if the yield is low or there are a lot of missing vines, the area to be harvested will be larger to fill a trailer, as a result, the weighing event (WE) will be allocated to a large harvest sector and the spatial resolution will be very low. More generally harvest sectors depend on the actual yield and the capacity of the trailers. In the case of lower yield and larger trailers, the spatial resolution will be lower than that observed in this study.

Another limitation of the approach is the impossibility to observe variability along the direction of the vine rows. This can be a significant drawback for blocks where environmental factors drive yield and grape quality variability along the rows, as this approach will not detect this source of variability.

The algorithm proposed in this work needs to be tested in more situations to account for particular harvest organizations; for example, it would be difficult to identify the proper trailer during a filling event (FE) with two trailers waiting side by side to be filled by the grape harvester. This specific case didn't occur during this study but it may lead to ambiguities in grape parameters reallocations. One solution would be to allocate

the measured parameters from both trailers to the grape harvester positions. The drawback would be that this would generate larger harvest sectors with a subsequent loss in spatial precision.

Concerning TDs installed on trailers, one perspective will be to test the relevance of TDs equipped with dual-frequency GNSS receivers, or EGNOS receivers. Compared to RTK-TDs, they are less accurate, a few decimeters for the dual frequency GNSS receivers, and 1 to 3 m accuracy for the EGNOS receivers. This lower accuracy for TDs on trailer (not on the grape harvester) should not be a problem for characterizing  $FE_s$  and  $WE_s$  given the threshold distance values ( $s_{FE} = 15$  m and  $s_{WE} = 10$  m) resulting from this study. One advantage of dual-frequency GNSS receivers and EGNOS receivers is to present a higher autonomy compared to RTK-TDs. This is a major advantage when it comes to limiting maintenance requirements during the harvest, in particular checking and recharging the batteries at a critical period in terms of work. An other-significant advantage is that these receivers are less expensive. This could be an interesting solution for larger structures (such as cooperatives) with several hundred hectares to harvest and dozens of winegrower members. Indeed, deploying the project on this scale requires a larger number of TDs, as several harvesting machines can be used, and a larger number of trailers will also be involved in the harvesting works. On this scale, any solution that reduces the unit price of each TD and simplifies site maintenance is an important aspect in facilitating adoption. Further experimentations are required to determine which technology is preferable; dual frequency or EGNOS. From a pure cost point of view, EGNOS receivers are to be preferred as they are the cheapest, but the risk of errors in characterizing  $FE_s$  and  $WE_s$  with this less precise technology needs to be tested and verified. Concerning TDs installed on harvester, RTK-TDs with centimeter accuracy seems to be the best option; first, because battery autonomy is not an issue as the TD can be connected to the power supply of the harvester, second, because the centimeter accuracy is important to detect vines rows which are harvested but also to detect accurately when the grape harvester is within blocks boundary and collecting grapes.

It should also be noted that the project, although tested in a real farm, uses a simple configuration with one grape harvester, three trailers and two different delivery sites. Scaling up to larger structures, such as those described in the previous section, necessarily involves a higher number of harvesting machines and trailers working all together on the site. Our algorithm has not been tested in this situation and its robustness still needs to be validated. In particular, it will be necessary to check whether the algorithm of the FE and WE detection does not generate assignment errors or indeterminations when the number of TDs increases on a harvesting site.

Regarding the information provided to the vineyard manager (VM); it appears that, although limited in terms of resolution, it is relevant enough to raise agronomic questions and lead to concrete proposals for improving vineyard management practices spatially. The data resulting from the study has led to the emergence of a rationale that, as far as we know, had never been considered in precision viticulture; nitrogen management based on YAN and yield. Indeed, in the literature, most precision viticulture studies aimed at optimizing nitrogen fertilization based on plant vigor measurements either estimated by remote sensing (Valloo et al., 2023) or using on-board sensors on machines (Sozzi et al., 2023). To our knowledge, this is the first time that a reasoning based simultaneously on YAN and yield is considered for different nitrogen fertilization strategies in precision viticulture. The approach permits to map many variables that are commonly measured at the winery. This gives access to new sources of information that are currently impossible to measure with on-board sensors. These sources of information can be very useful in helping the VM to

reconsider and optimize his farming practices as demonstrated in this study with nitrogen fertilization. This example remains simple in its approach, but the VM plans to take into account other sources of information, in particular vigor maps derived from remote sensing images, in order to refine certain decision rules. This shows the potential of this information, which makes sense to the VM in order to consider new management practices.

The VM adopted very quickly the maps generated here. Several reasons may explain this quick adoption: (i) harvest sectors are easy to handle and to understand for the VM, especially when compared to pixels or small zones resulting from high-resolution data which are sometimes more difficult to handle to define management zones, (ii) harvest sectors correspond to spatial units easily manageable since they fit with vine rows and mechanical interventions along the rows, (iii) the data generated are immediately understandable because they corresponds to the information and the units that the VM is used to (YAN in  $\text{mg l}^{-1}$ , potential alcohol in  $\% \text{ v v}^{-1}$ , etc.). For the VM, it requires much less effort to understand than some data commonly produced in precision viticulture like for example soil apparent resistivity in  $\text{ohm.m}$  or vegetation indices (NDVI, PCD, etc.). This rapid appropriation made it possible for the VM to consider experimentations on the farm based on the TDs in a second step. The overall idea of the VM is quite simple, since it aims at testing new management practices (inter row crops, soil tillage, manure, etc.) applied to a given number of rows forming a sector. The sector is then used to design the harvest operation. Since it is possible to get all the data (yield, pH, YAN, etc.) of this sector, it is then possible to have the results of the trial. The project enables on-farm experiments (Bramley et al., 2022) to be carried out, offering the possibility of simply measuring the characteristics of an experimental trial with classical harvesting operation.

## Conclusions

The work demonstrated the potential of a retro-fitted low-cost and easy to implement TD to monitor the whole harvesting process in viticulture in order to obtain low-resolution yield and harvest quality maps. Based only on the timing and the geolocation of all the vehicles (harvest trailers and grape harvester), it demonstrated the possibility to automatically reallocate, at the within-block level, the grape mass and harvest quality parameters collected at the winery. Despite their low resolution, the provided maps were relevant enough for the vineyard manager to question his management practices and propose new variable management practices on a unique application. The approach still needs to be tested over another season and if possible, at the level of a cooperative, in order to verify the robustness of the proposed algorithm before considering its deployment towards the wine industry.

**Acknowledgements** We acknowledge Christophe Clipet, Jérôme Cufi, Hugues Combes, Eric Thierry, Thomas Crestey, Pauline Faure and Théo Layre for their support in operating vehicles and collecting the block data during the project and Martine Catanese-Pons, Laure Haon and Christèle Cornier for the financial and administrative support of the study.

**Funding** This work has been funded by a grant from the Plant2Pro® Carnot Institute in the frame of its 2021 call for projects. Plant2Pro® is supported by ANR (Agreement Number 002401).

**Data availability** The data used to support the findings of this study are available from the corresponding author on reasonable request. An accurate description and access of some of these data are available in Gras et al. (2023).



## Declarations

**Conflict of interest** The authors declare that they have no known competing financial interests or personal relationships that could have appeared to influence the work reported in this paper.

## References

- Ancelin, J., Poulain, S., Peneau, S. (2022). «jancelin/centipede: 1.0», Zenodo, <https://doi.org/10.5281/zenodo.5814960>
- Arnaud, M., & Emery, X. (2000). *Estimation et interpolation spatiale: méthodes déterministes et méthodes géostatistiques (Spatial estimation and interpolation: deterministic and geostatic methods)*. Hermès.
- Báguena, E. M., Barreiro, P., Valero, C., Sort, X., Torres, M., & Ubalde, J. M. (2009). On-the-go yield and sugar sensing in grape harvester. *Precision agriculture '09, Proceedings of the 7th European conference on precision agriculture* (pp. 273–278). Wageningen Academic Publishers.
- Bayano-Tejero, S., Márquez-García, F., Sarri, D., et al. (2024). Olive yield monitor for small farms based on an instrumented trailer to collect big bags from the ground. *Precision Agriculture*, 25, 412–429. <https://doi.org/10.1007/s11119-023-10078-w>
- Birrell, S. J., Sudduth, K. A., & Borgelt, S. C. (1996). Comparison of sensors and techniques for crop yield mapping. *Computers and Electronics in Agriculture*, 14, 215–233. [https://doi.org/10.1016/0168-1699\(95\)00049-6](https://doi.org/10.1016/0168-1699(95)00049-6)
- Bramley, R. G. V., Le Moigne, M., Evain, S., Ouzman, J., Florin, L., Fadaili, E. M., & Cerovic, Z. G. (2011). On-the-go sensing of grape berry anthocyanins during commercial harvest: Development and prospects. *Australian Journal of Grape and Wine Research*, 17(3), 316–326. <https://doi.org/10.1111/j.1755-0238.2011.00158.x>
- Bramley, R. G., Song, X., Colaço, A. F., Evans, K. J., & Cook, S. E. (2022). Did someone say “farmer-centric”? Digital tools for spatially distributed on-farm experimentation. *Agronomy for Sustainable Development*, 42, 105. <https://doi.org/10.1007/s13593-022-00836-x>
- Chandra, R. V., & Varanasi, B. S. (2015). *Python requests essentials*. Packt Publishing Ltd.
- Ester, M., Kriegel, J., Sander, J., Xu, X. (1996). A density-based algorithm for discovering clusters in large spatial databases with noise. In: *Proceedings of the 2nd international conference on knowledge discovery and data mining*, pp. 226–231. <https://doi.org/10.5555/3001460.3001507>
- Gillies, S. et al., (2007). Shapely: Manipulation and analysis of geometric objects, Available at: <https://github.com/Toblerity/Shapely>
- Gras, J.-P., Brunel, G., Ducanhez, A., Crestey, T., & Tisseyre, B. (2023). Climatic records and within field data on yield and harvest quality over a whole vineyard estate. *Data in Brief*. <https://doi.org/10.1016/j.dib.2023.109579>
- Gutiérrez-Gamboa, G., Diez-Zamudio, F., Stefanello, L. O., Tassinari, A., & Brunetto, G. (2022). Application of foliar urea to grapevines: Productivity and flavour components of grapes. *Australian Journal of Grape and Wine Research*, 28, 27–40. <https://doi.org/10.1111/ajgw.12515>
- INRAE. (2019). Le réseau Centipede RTK—Centipede RTK (The Centipede RTK network—Centipede RTK). <https://docs.centipede.fr>
- Jordahl, K. (2014). GeoPandas: Python tools for geographic data. <https://github.com/geopandas/geopandas>
- Lachia, N., Pichon, L., Marcq, P., Taylor, J., & Tisseyre, B. (2021). Why are yield sensors seldom used by farmers? A French case study. In J. V. Stafford (Ed.), *Precision agriculture '19, Proceedings of the 12th European conference on precision agriculture* (pp. 745–751). Wageningen Academic Publishers.
- Longchamps, L., Tisseyre, B., Taylor, J., Sagoo, L., Momin, A., Fountas, S., et al. (2022). Yield sensing technologies for perennial and annual horticultural crops: A review. *Precision Agriculture*, 23, 2407–2448. <https://doi.org/10.1007/s11119-022-09906-2>
- McClymont, L., Goodwin, I., Mazza, M., Baker, N., Lanyon, D. M., Zerihun, A., & Downey, M. O. (2012). Effect of site-specific irrigation management on grapevine yield and fruit quality attributes. *Irrigation Science*, 30, 461–470. <https://doi.org/10.1007/s00271-012-0376-7>
- Momin, M. A., Grift, T. E., Valente, D. S., & Hansen, A. C. (2019). Sugarcane yield mapping based on vehicle tracking. *Precision Agriculture*, 20, 896–910. <https://doi.org/10.1007/s11119-018-9621-2>
- Pedregosa, F., et al. (2011). Scikit-learn: Machine learning in python. *Journal of Machine Learning Research*, 12, 2825–2830. <https://doi.org/10.48550/arXiv.1201.0490>
- Python-visualization. (2020). Folium, Available at: <https://python-visualization.github.io/folium/>

- QGIS Development Team. (2009). QGIS geographic information system. Open Source Geospatial Foundation. <http://qgis.org>
- Schueller, J. K., Whitney, J. D., Wheaton, T. A., Miller, W. M., & Turner, A. E. (1999). Low-cost automatic yield mapping in hand-harvested citrus. *Computers and Electronics in Agriculture*, *23*, 145–153. [https://doi.org/10.1016/S0168-1699\(99\)00028-9](https://doi.org/10.1016/S0168-1699(99)00028-9)
- Simmonds, M. B., Plant, R. E., Peña-Barragán, J. M., van Kessel, C., Hill, J., & Linquist, B. A. (2013). Underlying causes of yield spatial variability and potential for precision management in rice systems. *Precision Agriculture*, *14*, 512–540. <https://doi.org/10.1007/s11119-013-9313-x>
- Sozzi, M., Boscaro, D., Zanchin, A., Cogato, A., Marinello, F., & Tomasi, D. (2023). Variable-rate fertiliser application to manage spatial variability in a hilly vineyard of Prosecco PDO. *Precision agriculture '23, Proceedings of the 14th European conference on precision agriculture* (pp. 221–227). Wageningen Academic Publishers.
- Valloo, Y., Payen, S., Cornault, A., Vanrenterghem, R., Laurent, C., & Tisseyre, B. (2023). How to best compare remote sensing data versus proximal sensing data? *Precision agriculture '23, Proceedings of the 14th European conference on precision agriculture* (pp. 635–642). Wageningen Academic Publishers.
- Van Rossum, G., & Drake, F. L. (2009). *Python 3 reference manual*. CreateSpace.
- Verdenal, T., Spangenberg, J. E., Zufferey, V., Lorenzini, F., Spring, J. L., & Viret, O. (2015). Effect of fertilisation timing on the partitioning of foliar-applied nitrogen in *Vitis vinifera* cv. Chasselas: A 15 N labelling approach. *Australian Journal of Grape and Wine Research*, *21*, 110–117. <https://doi.org/10.1111/ajgw.12116>

**Publisher's Note** Springer Nature remains neutral with regard to jurisdictional claims in published maps and institutional affiliations.

Springer Nature or its licensor (e.g. a society or other partner) holds exclusive rights to this article under a publishing agreement with the author(s) or other rightsholder(s); author self-archiving of the accepted manuscript version of this article is solely governed by the terms of such publishing agreement and applicable law.